Uniform chemical shift scaling: Application to 2D resolved NMR spectra of rotating powdered samples

W. P. Aue, D. J. Ruben, and R. G. Griffin

Citation: The Journal of Chemical Physics **80**, 1729 (1984); doi: 10.1063/1.446928
View online: http://dx.doi.org/10.1063/1.446928
View Table of Contents: http://scitation.aip.org/content/aip/journal/jcp/80/5?ver=pdfcov
Published by the AIP Publishing

Uniform chemical shift scaling: Application to 2D resolved NMR spectra of rotating powdered samples

W. P. Aue,[a] D. J. Ruben, and R. G. Griffin
Francis Bitter National Magnet Laboratory, Massachusetts Institute of Technology, Cambridge, Massachusetts 02139
Children's Hospital Medical Center, Harvard Medical School, Boston, Massachusetts 02115

(Received 27 July 1983; accepted 21 November 1983)

Chemical shift scaling experiments which reduce the number and intensity of sidebands in high field magic angle sample spinning (MASS) spectra are described. They rely on the fact that the scaling pulse sequence reduces the effective size of the shift anisotropy, so that moderate speed spinning results in spectra devoid of sidebands of appreciable amplitude. In principle, the technique allows a realization of the full signal strength available in high field MASS spectra. In addition a number of other interesting features have emerged from the experiments. First, the problem of decoupling in the presence of a scaling sequence has been solved by arranging the rf field strengths to mismatch the Hartmann–Hahn condition. Second, it is shown that the scaling cycles used in the experiments are uniform over a wide frequency range with respect to both the scaling factor and the linewidth. Third, under certain conditions, the frequencies for scaling and spinning are about the same size and consequently new features appear in the spectra which we refer to as combination sidebands, combination artifacts, and zero and ν_r artifacts. We believe these features will be shared by many multiple pulse/MASS spectra. Finally, we demonstrate that a complete separation of centerbands and sidebands in high field MASS spectra is possible by incorporating chemical shift scaling into a two-dimensional experiment.

I. INTRODUCTION

High resolution solid state NMR methodology has expanded considerably over the last few years, and it is now clear that these techniques will be useful for investigating a wide variety of physical, chemical, and biological problems. Potentially, one of the most useful forms of solid state spectroscopy is a hybrid experiment involving magic angle sample spinning (MASS)[1,2] together with dilute spin double resonance.[3] The ubiquitous utility of this experiment arises from the fact that it yields well resolved spectra of arbitrary powder samples. This result is in contrast to that encountered in solid state spectroscopy of static specimens, where either single crystals or isotopically labeled compounds are generally required for unambiguous assignments of isotropic and anisotropic chemical shifts. Nevertheless, when these experiments are performed in high magnetic fields, or applied to samples exhibiting large shift anisotropies, certain interesting complications arise.

In general, the spin systems under investigation in these situations are governed by inhomogeneous Hamiltonians such as the anisotropic chemical shift. If the size of this interaction $\Delta\sigma$ (in Hz) is small compared to the spinner frequency ν_r, i.e., $\Delta\sigma < \nu_r$, then the static powder patterns collapse into single sharp lines at the isotropic frequencies of the chemically inequivalent spins, and the spectrum resembles a solution spectrum. In the opposite limit $\Delta\sigma \geqslant \nu_r$, the isotropic lines are flanked by sets of rotational sidebands at integral multiples of ν_r.[4–6] The number of sidebands and their intensities contain valuable information on the chemical shielding tensor elements, which can be extracted from the spectrum as long as sidebands and centerbands can be assigned.[7] However, the presence of these sidebands has two distinct disadvantages. First, since the signal of the observed nuclei is distributed among centerbands and sidebands, the sensitivity of the experiment is decreased. Second, in systems with several magnetically inequivalent nuclei, sidebands of one isotropic shift can overlap with centerbands or sidebands from adjacent resonances, and thus complicate the interpretation of the spectrum. In such situations, a technique which either attenuates or eliminates sidebands or separates sets of centerbands and sidebands is clearly desirable.

The simplest approach to identification of centerbands is to obtain MASS spectra at two or more spinner speeds. In this case the frequencies of the isotropic lines remain unchanged, whereas the sidebands move. Although this simple assignment method suffices in many cases, it is not generally applicable, and, recently, two alternative approaches have been proposed. In the first, the separation of sets of centerbands and sidebands is accomplished with a 2D resolved experiment,[8] in which the t_1-FID is sampled synchronously with the spinner. In the second (t_2) dimension the FID is sampled without restriction, and a 2D spectrum[9] is obtained displaying isotropic chemical shifts in ω_1 and isotropic together with anisotropic shifts in ω_2. Thus, a separation of the sets of centerbands and sidebands can be achieved. More recently, a one-dimensional method has been discussed, which allows identification of centerbands or any order of sidebands by coaddition of MASS spectra with systematically phase shifted sidebands.[10] This experiment is referred to as PASS and a variant of it called TOSS can be employed for total sideband suppression. All of the above methods have their disadvantages. In the one-dimensional PASS experiment, centerbands and sidebands are observed individually,

[a] Present address: Biozentrum der Universität Basel, Klingelbergstrasse 70, CH-4056 Basel, Switzerland.

 0021-9606/84/051729-10$02.10

and the sensitivity of this experiment is well below that obtained in an isotropic spectrum. A similar statement is applicable to TOSS, at least in the situation where there are large numbers of sidebands present. In this case, most of the sideband signal is scrambled and thus the observed centerband intensity is very nearly that observed in the normal MASS spectrum. Finally, the 2*D* experiment does not yield a complete separation of centerbands and sidebands in all cases, a point which will be discussed in more detail below.

The deficiencies of the available methods provided the impetus for the experiments described in this article. Our present approach makes use of the fact that both isotropic and anisotropic chemical shifts can be reduced to a predetermined size by relatively simple multiple pulse sequences, an effect known as chemical shift scaling.[11] A further and almost complete narrowing is then accomplished with sample rotation. This approach is fundamentally different from that taken by Dixon and co-workers.[10] In this latter case, no attempt is made to reduce the size of the chemical shift interaction. Instead, as mentioned above, the phases of the sidebands are systematically manipulated so that they are either observed individually, or they are partially refocused to yield a centerband with reduced intensity.

In connection with MASS experiments, chemical shift scaling can in principle be employed in at least three different ways which permit assignment and/or separation of centerbands and sidebands.[12] In the first, the shift anisotropies are scaled so that the condition $\Delta\sigma_{sc} \leqslant \nu_r$ is satisfied, where the subscript refers to a scaled $\Delta\sigma$. The spectrum is then dominated by isotropic resonances which may be flanked by weak sidebands. Second, if the isotropic shifts are scaled so that their frequency dispersion $\Delta\delta$ satisfies $\Delta\delta < \nu_r$, then synchronous sampling may be incorporated into the experiment, and the result is a spectrum devoid of sidebands. The signal-to-noise advantage to this approach is clear; specifically, any signal intensity originally resident in the sidebands is transferred predominantly to the centerband and a gain in sensitivity is achieved. When synchronous sampling is possible the transfer is complete. Finally, even if the constraint $\Delta\delta \leqslant \nu_r$ is not satisfied, it is still possible to employ synchronous sampling together with scaling in a profitable manner.

As mentioned above, we previously described a 2*D* experiment in which the magnetization is sampled synchronously with the rotor during t_1 and without restriction during t_2.[8] The resulting 2*D* spectrum displays isotropic shifts alone in ω_1, but both isotropic and anisotropic shifts together in ω_2. Naively, it might be predicted that aliasing would be a *severe* problem in such a spectrum because of the limited bandwidth in the ω_1 dimension. For example, in ^{13}C spectra obtained at superconducting fields, the spectral width is about an order of magnitude greater than commonly available spinning frequencies. Thus, lines from $-CH_3$ and $-CH_2-$ groups might be aliased into the carbonyl/aromatic region of the spectrum. While it is true that aliasing will occur in the ω_1 dimension, it is also true that methyl and methylene resonances will never be aliased into the aromatic and carbonyl region. Specifically, the ω_2 dimension contains redundant information, namely the isotropic shift, and because of this the methyl and methylene lines appear in their normal "upfield" region, well separated from the aromatic and carbonyl lines. An example explicitly demonstrating this point is included below. Nevertheless, in certain cases the 2*D* experiment will not yield a complete separation. In particular, any two resonances which have isotropic shifts δ_i and δ_j separated by $n\nu_r$ will appear at the same frequency in ω_1. Furthermore, if the sideband patterns from these two lines overlap, then these patterns will not be separated in the two-dimensional spectrum. By introducing chemical shift scaling into the ω_1 dimension of the experiment, it is possible to circumvent this situation—i.e., the isotropic shifts are scaled so that $\nu_r > \delta_{i_{sc}} - \delta_{j_{sc}}$. With this modification, the two-dimensional experiment becomes generally applicable.

In the following section uniform chemical shift scaling is briefly reviewed and several schemes for performing scaling in the simultaneous presence of heteronuclear decoupling are discussed. In Sec. IV we present experimental results obtained with the various decoupling schemes. They indicate that the optimum method for performing these experiments probably employs cw decoupling together with a scaling sequence chosen to mismatch the Hartmann–Hahn condition. In addition, we describe in this section some artifacts which appear in scaled MASS spectra. We believe that these artifacts are a general feature of multiple pulse/MASS experiments. The last section discusses the 2*D* resolved MASS experiment described above from which both isotropic and anisotropic chemical shifts may be obtained. Finally, multiple pulse NMR experiments are regarded in many quarters as difficult to implement. For this reason we have also included an Appendix with a detailed description of the procedures necessary for performing chemical shift scaling in rotating samples.

II. UNIFORM CHEMICAL SHIFT SCALING IN ROTATING SOLIDS

The fact that multiple pulse trains can be employed to selectively attenuate certain terms in a nuclear spin Hamiltonian is well known. One of the earliest descriptions of this phenomenon involved scaling chemical shifts in liquids, and was appropriately christened the "chemical shift concertina."[11] Briefly, a train of phase alternated pulses—e.g., $x\bar{x}$—is applied to the sample, and the magnetization is observed stroboscopically in the time intervals between the pulses. The result is that the spectrum width arising from linear interactions, such as the chemical shift, is reduced in size by a factor q, the scaling factor. Bilinear terms in the Hamiltonian—homonuclear J couplings—are unaffected by the simple pulse train. The size of q is of course governed by a number of factors including the nutation angle, the pulse spacing, and the cycle time. We will discuss this further below.

An important consideration in these experiments is that the scaling factor be constant over the spectral width of interest. In the original work of Ellett and Waugh,[11] a so-called separated scaling sequence was employed. As shown in that paper and elsewhere, this sequence is particularly sensitive to resonance offset effects. More recently, the question of uniformity of scaling has been considered in detail in connec-

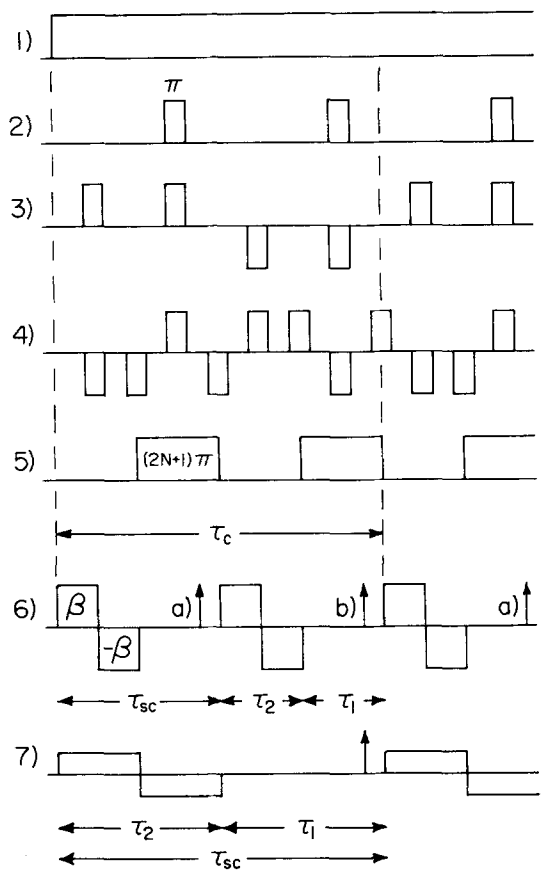

FIG. 1. rf pulse schemes, which were investigated for uniform scaling (6,7) and efficient heteronuclear decoupling (1)–(5). The different decoupling schemes acting on the I spins are (1) on-resonance cw decoupling; (2) two π pulses per scaling/decoupling cycle τ_c; (3) four phase alternated π pulses per τ_c; (4) eight phase π pulses per τ_c; (5) time shared decoupling. The flip angles for complete heteronuclear decoupling with an isolated I–S spin pair are indicated. Scaling sequences (6) and (7) acting on the S spins feature trains of joined pulses of opposite phases. In (6), the rf field in frequency units is the same as for the I spins, i.e., the Hartmann–Hahn condition is fulfilled. The basic scaling cycle τ_{sc} has half the length of τ_c. Samples (a) indicated with vertical arrows, are taken once every scaling/decoupling cycle τ_c. Sampling once per basic scaling cycle τ_{sc} [samples (a) and (b)] does not produce artifacts and improves sensitivity. Sequence (7) uses a reduced rf field to quench cross polarization. Since flip angle and duty ratio of the scaling sequence have to be maintained to obtain the same scaling factor, pulse timing has to be adjusted accordingly.

tion with scaling of heteronuclear J couplings in liquids, and it was shown that for a given rf power level, a joined sequence depicted in (6) and (7) of Fig. 1 results in improved performance.[13–15] Similar sequences though not optimized for uniformity have been employed in chemical shift relaxation studies of static solids.[16] In the experiments discussed here we have always employed the joined scaling sequence.

The scaling factor for the pulse trains shown in Fig. 1 can be obtained from average Hamiltonian theory.[17–19] The complete calculations for a Hamiltonian containing terms corresponding to isotropic chemical shifts and heteronuclear J couplings have been described elsewhere.[15] For the present we simply quote the result of zeroth order average Hamiltonian calculations applicable to the isotropic part of the chemical shift interaction which is

$$q^{(0)} = \frac{1}{\tau_{sc}} \left[\tau_1^2 + 2\tau_2^2 (1 - \cos\beta)/\beta^2 + 2\tau_1\tau_2 \sin\beta/\beta \right]^{1/2},$$

where τ_1, τ_2, and τ_{sc} are the time intervals shown in Fig. 1 and β is the nutation angle. The choice of these parameters determines the scaling factor and it can in principle be adjusted between 0 and 1. Parameters for the joined scaling sequence shown in Fig. 1, which are optimized for uniformity and sensitivity to rf inhomogeneity are given in Ref. 14 for different scaling factors and rf field strengths. The scaling factor is determined by the duty ratio and flip angle, and therefore optimized scaling sequences can be recomputed for an arbitrary rf field strength from the tables in the above reference.

Thus far, we have only considered the effect of the S spin scaling sequence on the Hamiltonian. However, in a solid we also must suppress both the homo- and heteronuclear dipolar interactions—i.e., the I–I and I–S couplings. In a normal MASS experiment, this is accomplished most efficiently with cw irradiation of the I spins. In particular $\mathscr{H}_{IS} \propto I_z S_z$ and the cw irradiation at the I spin frequency induces a time dependence in I_z. If the decoupling field is sufficiently large, then $\bar{\mathscr{H}}_{IS} = 0$ and well resolved spectra are observed. This decoupling scheme is illustrated in (1) of Fig. 1. The case considered here is complicated by the fact that S_z is now also time dependent due to the scaling sequence, and as a consequence $\mathscr{H}_{IS} \propto I_z(t) S_z(t)$ and will not vanish in general. A similar situation has been encountered previously by Mehring[20,21] and Haeberlen[19,22] in ^{23}Na–^{19}F and ^{1}H–^{19}F experiments and more recently by Reimer and Vaughan[23,24] in connection with ^{13}C–^{1}H studies.

The simplest approach to this problem is to arrange the I and S spin rf pulses so that they do not overlap, and the S and I spin operators can be treated separately. For example, in the ^{23}Na ^{19}F experiments of Mehring *et al.*[20] a single π pulse at the ^{23}Na frequency was placed in one of the 2τ windows of the ^{19}F WAHUHA sequence. This approach is analogous to decoupling sequence (2) and scaling sequence (6) in Fig. 1 and proved to be adequate for decoupling of ^{23}Na from ^{19}F. Haeberlen and co-workers[22] have successfully used sequence (3) of Fig. 1 in ^{1}H–^{19}F experiments. It is superior to sequence (2) since it eliminates all even and odd correction terms to the average Hamiltonian. Sequence (4) of Fig. 1 is a variant of sequence (3), which was supposed to increase the average rf power, and finally sequence (5) was designed to avoid simultaneous rf fields on the I and S spins. Recently, Reimer and Vaughan have described ^{1}H–^{13}C experiments in which they employed a sequence similar to (5).

In all of the previous cases where these decoupling schemes were successfully employed, the resolution requirements were relatively modest. For example, Mehring *et al.* and Reimer and Vaughan were concerned exclusively with powder samples and in such cases linewidths of 5 or even 10 ppm are tolerable. In the single crystal KHF_2 investigation by Van Hecke *et al.*, the ^{19}F decoupled ^{1}H linewidths were $\sim$20 ppm. In MASS spectra considered here linewidth contributions of 0.5 ppm are easily noticed, and we have found that schemes (2)–(5) all result in significantly larger contribu-

tions to the linewidths. Although we have not performed a detailed analysis of this point, we believe it is primarily due to three causes. First, pulse decoupling is inherently less efficient than cw decoupling, and second, the schemes (2)–(5) are designed to eliminate heteronuclear rather than homonuclear interactions. Since the latter are clearly present in the samples we have investigated, we should expect some dipolar broadening which is not eliminated by the sample rotation. Thirdly, when the rf fields are matched to the Hartmann–Hahn condition[25,26] then cross polarization occurs when both fields are present.

The solution to the decoupling problem which we propose utilizes cw irradiation at the I spin frequency and a scaling sequence with attenuated rf pulses. The size of the S spin rf field is simply attenuated so as to mismatch the Hartmann-Hahn condition as is shown in sequence (7) of Fig. 1. This approach yields spectra whose lines are in most cases narrower than those observed in conventional MASS spectra. Experimental results verifying this fact are given in Sec. IV.

TABLE I. Comparison of linewidths observed in normal MASS spectra with those observed using the different decoupling schemes illustrated in Fig. 1. In all cases scaling was accomplished with sequence (6) of Fig. 1, e.g., with approximately matched Hartmann–Hahn fields. Samples consisted of 90% enriched $Na(CH_3CH_2^*CO_2)$, $Na(CH_3^*CH_2CO_2)$, $Ca(^*CHO_2)_3$, and $Na(^*CH_3CO_2)$, where the asterisk denotes the labeled position. The experimental parameters were: $\gamma H_1(^{13}C) = 56$ kHz, $\gamma H_1(^1H) = 66$ kHz, $q = 0.5$, $\tau_{sc} = 65\ \mu$s, and $\nu_r = 2.5$ kHz. The rf field, q, and τ_{sc} correspond to 270° scaling pulses (see Table I of Ref. 14). Resonance offsets were 6 kHz for CO_2^- and $-CH_2-$ groups and 2 kHz for CH and $-CH_3$ groups.

Decoupling sequence	Duty factor	Linewidths (FWHH) in Hz for $-CO_2^-$	$-CH^-$	$-CH_2^-$	$-CH_3$
(1) cw	1.00	80	440	1100	180
(2) 2 pulse	0.12	100	210	2000	100
(3) 4 pulse	0.23	125	240	1880	150
(4) 8 pulse	0.47	105	290	1470	160
(5) Time shared	0.58	60	130	580	90
Normal MASS	1.00	50	140[a]	120	65

[a] Two overlapping lines.

III. EXPERIMENTAL

The ^{13}C and ^{15}N NMR spectra reported here were obtained on a home-built pulse spectrometer operating at 74.9 MHz for ^{13}C, 29.8 MHz for ^{15}N, and 294 MHz for ^1H. Two different MASS probes were employed in the experiments, both of which used Andrew-Beams type rotors.[2] In the ^{13}C experiments the maximum rf fields obtainable were close to 65 kHz, whereas in the ^{15}N experiments the maximum fields amounted to about 74 kHz. The decoupling field on the protons was around 70 kHz. Spinner frequencies were constant to $\leqslant$10 Hz over a 24 h period. Most of the spectra were obtained from ^{13}C or ^{15}N enriched samples which were purchased from commercial sources (Merck Isotopes St. Louis, MO; Stohler Isotopes, Waltham MA; or Kor Isotopes, Cambridge MA). The ^{13}C labeled compounds include sodium propionate, sodium acetate, glycine, and calcium formate. For the ^{15}N experiments we employed Gly·Gly·HCl·H_2O with both nitrogens labeled.

IV. RESULTS AND DISCUSSION

The performance of the various scaling/decoupling schemes illustrated in Fig. 1 was investigated with two straightforward sets of experiments. First, the efficiencies of the decoupling schemes illustrated in Fig. 1 were compared by measuring linewidths in scaled ^{13}C spectra. Second, we investigated the uniformity of the scaling factor, i.e., the magnitude of the scaling factor as a function of frequency offset.

A. Decoupling

The results obtained with the different decoupling schemes illustrated in Fig. 1 are assembled in Table I. In order to facilitate meaningful comparisons, the parameters employed in these experiments were maintained constant and are included in the legend of the table. An important point concerning the results in Table I is that these data were obtained with proton and ^{13}C fields which nearly matched the Hartmann–Hahn condition. Inspection of the linewidth data shows that substantial line broadening occurs with all of the decoupling schemes except for nonprotonated carboxyl groups and $Ca(CHO_2)_2$, where the proton spin density is relatively low. In the case of $-CH_2-$ groups, where decoupling requirements are most stringent, linewidths of 0.6–2 kHz are observed. Thus, the pulsed decoupling schemes shown in Fig. 1, as well as cw decoupling in the presence of S spin fields which match the Hartmann–Hahn condition, appear to be of little utility for the high resolution MASS experiments considered here.

Nevertheless, the data in Table I do show certain trends which suggest ways in which the decoupling schemes could be improved. For example, with the pulsed decoupling schemes the linewidths are approximately inversely proportional to the rf duty factor. This is best illustrated by the $-CH_2-$ data, where the linewidth decreases from 2 to 0.58 kHz as the duty factor is raised from 0.12 to 0.58. Extrapolation of these results suggests that cw irradiation would be the most efficient decoupling scheme, which is not an unexpected result. Concurrently, cross polarization during the scaling pulses must be avoided. These two features can be incorporated into the scaling experiment by simply reducing the rf power at the S spin frequency, while maintaining the decoupling field at its full strength. Specifically, the MASS scaling experiment should employ sequence (1) for decoupling and (7) for chemical shift scaling.

In Table II we have assembled linewidth data for two samples which illustrate the success of this approach. In the top half of the table are shown results from ^{13}C spectra of glycine for two different scaling factors. It can be discerned that the $-CO_2^-$ linewidth is reduced approximately in proportion to the scaling factor, as should be the case for inhomogeneously broadened lines. Moreover, the $-CH_2-$ line, which is the most difficult case to decouple, can be scaled without significant line broadening. In the lower half of Table II are shown data from ^{15}N spectra of Gly·Gly·HCl·H_2O

TABLE II. Comparison of linewidths obtained in normal MASS spectra with those observed when the S spin scaling pulses were attenuated to mismatch the Hartmann–Hahn condition. Resonance offsets in the ^{13}C and ^{15}N experiments were ± 2 and ± 1.13 kHz, respectively. The S spin scaling fields are given in percent of the field necessary to match the Hartmann–Hahn condition.

Sample	Scaling rf field	q	τ_{sc} (μs)	Linewidths (FWHH in Hz)	
Glycine–^{13}C				CO_2^-	$-CH_2^-$
	43%	0.5	125	40	115
	43%	0.3	94	28	105
Normal MASS				60	110
Gly · Gly · HCl · H_2O–^{15}N				>NH	$-NH_3^+$
	57%	0.5	86	70	30
	49%	0.5	100	40	28
	40%	0.5	120	24	22
	32%	0.5	150	24	20
Normal MASS				26	22

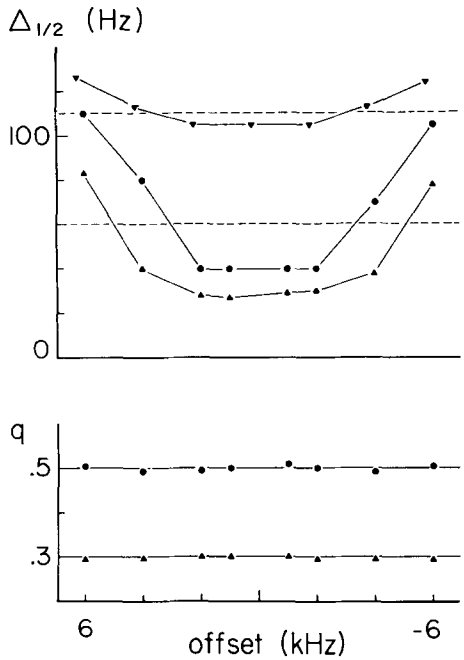

FIG. 2. Experimental scaling factors (bottom) and linewidths (top) as a function of the frequency offset in an experiment with cw decoupling and Hartmann–Hahn mismatched scaling on glycine. The triangles indicate the results for an experiment with $q = 0.30$ on the $-CO_2^-$ and the $-CH_2^-$ groups. The rf fields were 66 and 28 kHz for protons and ^{13}C. The scaling cycle time τ_{sc} was 94 μs and the spinner rate was 2.66 kHz. Over an offset range of 12 kHz the scaling factor compares very well with the on-resonance value of 0.300, which is indicated with the solid line. The linewidths are compared to those in a conventional MASS experiment, represented with dashed lines. Line narrowing is achieved over a range of 10 kHz for CO_2^- (▲) and 7 kHz for $-CH_2^-$ (▼). The full circles give the results for $q = 0.5$ on CO_2^-. Except for a cycle time of 125 μs, the above parameters were used. Again, scaling is uniform over 12 kHz, and line narrowing is obtained over 6 kHz. The data points for the linewidths have been connected by straight lines to enhance visibility.

which illustrate the degree to which the Hartmann–Hahn condition must be mismatched. In this set of experiments both the scaling factor and decoupling fields were maintained constant. The ^{15}N rf field was then attenuated and the scaling cycle time was adjusted accordingly. The results indicate that the best resolution is observed where the rf fields for the two nuclei differ by more than a factor of 2.

B. Uniformity

As mentioned above uniformity of scaling—i.e., offset independence of the scaling factor—is essential if quantitative chemical shift information is to be extracted from the scaled MASS spectra. Moreover, it is well known that linewidths in multiple pulse—i.e., scaling—experiments exhibit offset dependences. This could lead to line broadening, particularly in the wings of scaled spectra, or when large shift tensors are studied, to improper scaling of the rotational sideband intensities. Accordingly, we have performed several different experiments using the scaling sequences of Fig. 1 to investigate these effects in MASS spectra. The results demonstrate that the uniformity of the joined scaling cycle is clearly satisfactory.

In Fig. 2 are shown plots of the scaling factor q and linewidths as a function of frequency offset, and in Tables III and IV, are assembled some data pertinent to these plots. All of these data were obtained from carboxyl and methylene ^{13}C enriched samples of glycine, and the rf fields were adjusted to mismatch the Hartmann–Hahn condition. As shown in the bottom half of Fig. 2, the uniformity of the scaling sequence is quite good for the two values (0.3 and 0.5) investigated. Specifically it is within 2% over ± 6 kHz, which agrees quite well with the uniformity predicted in the tables of Ref. 14. Note that Table II also contains data for the $-{}^{15}NH_3^+$ line in Gly·Gly·HCl·H_2O and again a uniformity of within 2% is achieved over ± 6.4 kHz.

The top half of Fig. 2 illustrates the offset dependence of the linewidths observed with $q = 0.3$ and 0.5 and also compares the scaled linewidths with those obtained in normal MASS experiments. With $q = 0.3$ the linewidths are reasonably constant over an offset range of ± 4 kHz. With $q = 0.5$ a somewhat stronger offset dependence was observed, but for ± 3 kHz it was still below the 50% level of line broadening which we consider tolerable. In the case of $-{}^{15}NH_3^+$ in Gly·Gly·HCl·H_2O, we obtained similar results as are shown in Table IV. In summary, the results in Fig. 2 and Tables III and IV indicate that scaling uniform to ± 2% over ± 6 kHz (160 ppm) can be achieved for ^{13}C with the rf fields we employed. The offset range with $\leqslant$50% line broadening is ± 5 kHz for $q = 0.3$ and ± 3 kHz for $q = 0.5$. In the case of ^{15}N,

TABLE III. Uniformity of scaling observed in ^{13}C and ^{15}N MASS spectra. The data was obtained from ^{13}C labeled glycine and ^{15}N labeled Gly Gly · HCl · H_2O. The numbers in parentheses in the resonance offset ($\Delta\omega$) column indicated the fraction of inverse cycle time over which uniformity was observed.

Sample	q	τ_{sc} (μs)	$\Delta\omega$ (kHz)	Uniformity (%)	Calculated uniformity
$-CO_2^-$, $-CH_2-$	0.3	94	± 6 (0.56)	1.7	1.3
$-CO_2^-$	0.5	125	± 6 (0.75)	2.0	2.0
NH_3^+	0.5	150	± 6.4 (0.96)	2.0	2.1

TABLE IV. Linewidths in scaled spectra as a function of frequency offset. The number in parentheses in the resonance offset column indicate the fraction of the inverse cycle time over which the linewidths were maintained.

Sample	q	Line broadening	$\Delta\omega$ (kHz)
$-CO_2^-$	0.3	<50%	±5 (0.47)
$-CH_2^-$	0.3	<50%	±8 (0.75)
$-CO_2^-$	0.5	min	±2 (0.25)
		<50%	±3 (0.38)
$-NH_3^+$	0.5	min	±4.5(0.68)
	0.5	<50%	±5.2(0.78)

2% uniformity was achieved over ± 6.4 kHz (430 ppm) and the offset range with ⩽50% line broadening is ± 5.2 kHz.

It should be pointed out that the rf fields we employed for scaling were rather modest (< 30 kHz) and the cycle times τ_{sc} were ~ 100 μs or longer. In fact, these parameters resemble solution more than solid state NMR experiments. Moreover, the cycle time, which is largely dictated by the pulse widths, determines the offset range over which uniform scaling can be maintained. As can be seen from Tables III and IV, uniformity of 2% is achieved for ^{13}C at about $0.7/\tau_{sc}$. Thus, in order to increase the useful offset ranges it is necessary to increase the rf field strengths. A modest increase in the rf field strength would permit uniform scaling over the ± 9 kHz (250 ppm) range characteristic of ^{13}C chemical shifts at our operating field of 7 T.

For theoretical and experimental reasons, the entire range of scaling factors between 0 and 1 is not accessible with the same favorable results. In particular, the optimal performance of the joined scaling cycle occurs for $q = 0.2$–0.6. For q outside this range, the uniformity and sensitivity to rf inhomogeneity degrade rapidly. However, as will be seen below, values of $q = 0.5$ are sufficient to reduce sideband intensities to acceptably low values. For example, aromatic and carbonyl shift anisotropies range from 150–200 ppm and with $q = 0.5$ and $\nu_r \approx 2$–2.5 kHz, the sidebands contain about 5%–10% of the intensity resident in the centerband. At higher fields—i.e., 12 T— scaling factors in the neighborhood of 0.3 are desirable and the plots in Fig. 2 attest to their feasibility.

The effect of scaling on rotational sideband intensities is illustrated in Fig. 3 which shows ^{31}P spectra of barium diethyl phosphate. This compound was chosen since it exhibits a rather large shift anisotropy (~22 kHz), and the spectra were taken at a low spinning speed of 1.88 kHz in order to increase the number and intensity of the sidebands. The bottom spectrum in this figure was obtained with a normal MASS experiment and shows eight sets of rotational sidebands, in addition to the centerband. The middle spectrum was recorded with $q = 0.4$ and a scaling rate of 15.65 kHz. Under these conditions the number of sideband sets is decreased to four and the centerband is now the dominant line in the spectrum. In order to demonstrate the scaling uniformity we show in the top trace a computer simulation of the scaled spectrum. Input parameters for this simulation consisted of the rigid lattice BDEP tensor elements as determined by Herzfeld *et al.*[27] reduced by the scaling factor and

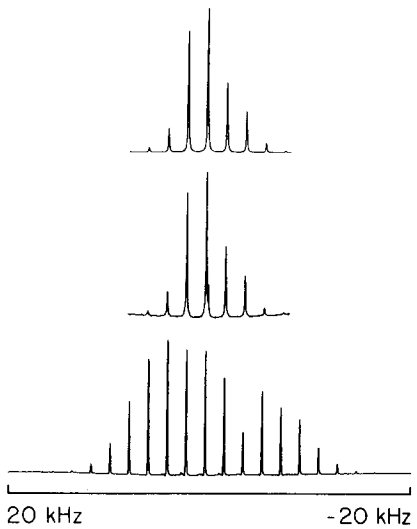

FIG. 3. Proton decoupled ^{31}P MASS spectra of barium diethyl phosphate. Bottom: Normal MASS spectrum obtained at $\nu_r = 1.88$ kHz, RD = 5 s. Middle: MASS spectrum scaled with $q = 0.4$ ($\nu_{sc} = 15.65$ kHz) illustrating the reduced number of sidebands. The centerband is now the most intense line in the spectrum. Top: MASS spectrum calculated assuming the rigid lattice BDEP tensor values scaled by 0.4. There is excellent agreement between the calculated and measured sideband intensities.

the spinning speed. As is clear from Fig. 3 there is excellent agreement between the experimental and calculated line intensities.

C. Combination sidebands, combination artifacts, and zero and ν_r artifacts

In the chemical shift scaling experiments described here three different averaging processes are present simultaneously: heteronuclear cw decoupling with rf field strengths of about 70 kHz, scaling at frequencies $\nu_{sc} = 1/\tau_{sc} \approx 5$–$15$ kHz, and MASS at $\nu_r \approx 1.5$–4.0 kHz. When the characteristic frequencies of these three processes are much different from one another, then they can be treated independently.[28] The frequencies associated with decoupling and scaling or MASS clearly fall into this regime. However, when the frequencies of the latter two averaging processes become the same size then certain interesting features appear in the spectra. In particular, one process can modulate the other, and under certain circumstances additional lines or sidebands are observed. We refer to these lines as "combination sidebands" and "combination artifacts."

A series of ^{15}N spectra illustrating the combination sidebands and artifacts are shown in Fig. 4. The sample employed in these experiments was Gly·Gly·HCl·H_2O and the spectra were taken as a function of ν_r for $\nu_{sc} = 6.67$ kHz and $q = 0.5$. As a consequence, ν_{sc}/ν_r varied from 1.67 ($\nu_r = 4.00$ kHz), to 2 ($\nu_r = 3.33$ kHz), to 2.49 ($\nu_r = 2.68$ kHz). The line on the right-hand side of the spectrum corresponds to the $-^{15}NH_3^+$, while the pattern on the left-hand side arises from the $>{}^{15}NH$ group.

At the highest spinning speed of 4 kHz the spectrum consists of two resonances corresponding to the isotropic shifts of the > NH and $-NH_3^+$ groups. The NH resonance is flanked by very weak sidebands at ± 1.33 kHz. However, as

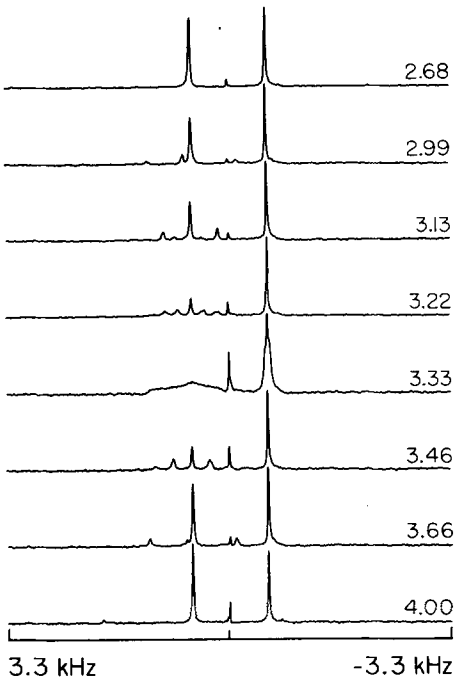

FIG. 4. ν_r artifacts, combination artifacts and combination sidebands in a scaled spectrum of double ^{15}N labeled glycylglycine. The rf fields were 74 and 28 kHz for proton and ^{15}N. Scaling factor and scaling rate were kept constant at $q = 0.50$ and $\nu_{sc} = 6.67$ kHz, while the spinner rate varied between 2.68 and 4.00 kHz as indicated on the single traces. Whereas the top trace shows the ν_r artifact at zero frequency only, the lower traces show combination sidebands flanking the $>$NH line (left) at intervals of $\nu_{sc} - 2\nu_r$ and combination artifacts at integer multiples of $\nu_{sc} - 2\nu_r$. For $\nu_r = 3.33$ kHz ($\nu_{sc} = 2\nu_r$), distorted powder line shapes are obtained instead of patterns with sharp spinning sidebands.

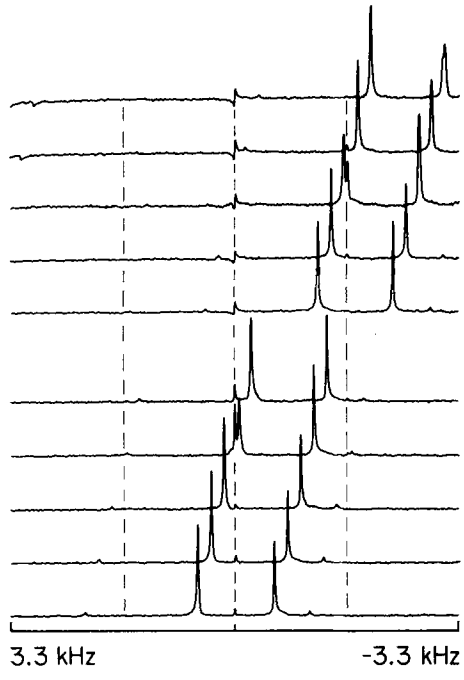

FIG. 5. ν_r artifacts in a scaled spectrum of doubly ^{15}N labeled glycylglycine. The rf fields were 74 and 28 kHz for protons and ^{15}N. The scaling factor was $q = 0.50$, the scaling rate ν_{sc} 6.67 kHz and the spinner rate $\nu_r = \nu_{sc}/4 = 1.67$ kHz. The offset of the resonances was changed to cover a range of 7.2 kHz. The broken lines indicate the positions of the ν_r artifacts, which show up as soon as a resonance moves by. Line broadening becomes apparent for maximum offset (top trace).

the spinner speed is reduced to 3.66 or 3.46 kHz additional strong sidebands appear in the spectra. Note that at $\nu_r = 3.33$ kHz ($\nu_{sc}/\nu_r = 2$) a distorted powder line shape is observed while at still lower spinning speeds the combination sidebands reappear. The spacing of the combination sidebands observed in all of the spectra of Fig. 4 turns out to be $\pm |\nu_{sc} - 2\nu_r|$. Note also that they are never observed for the $-$ $^{15}NH_3^+$ line, probably because of the very small shift anisotropy of this group. Finally, when $\nu_{sc}/\nu_r \gtrsim 3$ these combination sidebands are not observed. The combination artifacts are also illustrated in the spectra of Fig. 4 at $\nu_r = 2.99$ and 3.66 kHz. They appear as small additional lines downfield of the $>$ ^{15}NH signal. This class of modulation sidebands was observed at multiples of ν_{sc}–$N\nu_r$ ($1 \leqslant N \leqslant 3$) for $\nu_{sc}/\nu_r \lesssim 3$ in various cases. Their appearance is the same as that of the ν_r artifacts, which are described in more detail below. As mentioned above we believe the origin of these sidebands is the fact that we have two processes—spinning and scaling—modulating the NMR signals at very nearly the same frequencies. Thus, what appears in the NMR spectra are lines at the difference frequencies. We postpone until a future publication a complete theoretical explanation of these sidebands. For the moment, we note that the regime in which they appear ($\nu_{sc}/\nu_r \approx 2$) is easy to avoid experimentally, and as mentioned above when $\nu_{sc}/\nu_r > 3$ the combination sidebands and combination artifacts are no longer observed. Finally, we should mention that powder patterns like those seen at $\nu_r = 3.33$ kHz were first reported by Lippmaa and co-workers[4] and more recently by Yarim-Agaev *et al.*[30] and Bax *et al.*[31]

In addition to combination sidebands and combination artifacts we have also observed another class of extra lines in scaled MASS spectra which we refer to as zero and ν_r artifacts. In particular, when an NMR signal occurs near either zero or multiples of $\pm \nu_r$ and if the pulse sequence satisfies certain criteria, then part of the NMR signal intensity is transferred to this artifact. Figure 5 shows a series of ^{15}N spectra obtained from Gly·Gly·HCl·H_2O which illustrates these artifacts. Note that when the $>$ ^{15}NH line (on the left-hand side of each spectrum) is far from ν_r or zero, then the spectra contain two lines as expected. However, as the offset frequency is changed and the $>$ ^{15}NH resonance moves near to either $-\nu_r$ or zero, then part of the signal intensity is transferred into an extra line appearing at one of these frequencies. Finally, we should also mention that we have recently observed these artifacts in ^1H multiple pulse/MASS spectra.[29] Thus, they appear to be a general feature of these sorts of experiments.

At the moment we believe the most likely sources of the artifacts are pulse width and/or phase errors in the scaling pulse train. First, computer simulations to be described in another paper show that when the two pulses of the scaling pulse train are perfect, then there is no artifact present. However, when a 5° error is deliberately inserted into the calculation—e.g., scaling with 270°_x, $265^\circ_{\bar{x}}$, rather than 270°_x, $270^\circ_{\bar{x}}$—then the artifacts appear.[29] Furthermore, we have observed experimentally that when the relative rf phases of the

two scaling pulses are misadjusted, then the size of the artifact increases. Similar results are observed when the pulse widths and phases are misadjusted in ^1H multiple pulse/MASS spectra. Finally, it should be mentioned that the zero artifact described here is not related to the effects recently discussed by DiVerdi and Opella.[32] The pulse sequences used by these authors result in no improvement in either the size or frequency dependence of the zero and ν_r artifacts over the sequences used here. This is predicted by the computer simulations mentioned above and has been confirmed experimentally.

Finally, the spectra of Fig. 5 illustrate another important point alluded to in the Introduction. Specifically, we stated that a TOSS experiment refocuses only part of the spectral intensity residing in the sidebands into the centerband. In contrast, with scaling the effective size of the shift tensor is reduced, and therefore the spinning speed required to narrow the spectrum to primarily a centerband containing the full signal is considerably lower. The spectra of Fig. 5 present an experimental confirmation of the point. Specifically, at $\nu_r = 1.67$ kHz, where these spectra were obtained, the $> {}^{15}NH$ shift spectrum consists of a centerband containing only about 60% of the spectral intensity.[33] In contrast, the very small shift anisotropy of the $- {}^{15}NH_3^+$ group (< 10 ppm) results in this line not showing any significant sideband amplitude and it thus serves as an intensity standard. When the $> {}^{15}NH$ spectrum is scaled with $q = 0.5$, the result is that essentially the full intensity of the $> {}^{15}NH$ signal now resides in the centerband. That this is the case can be ascertained by noting that the $> {}^{15}NH$ and $- {}^{15}NH_3^+$ lines are of equal intensity except when a zero or ν_r artifact is present.

D. 2*D* resolved MASS spectroscopy

In the previous discussion much of our attention was focused on reducing a MASS spectrum containing rotational sidebands to a solution-like spectrum displaying predominantly the isotropic chemical shifts. While such liquid-like spectra are relatively easy to analyze and quite useful, they nevertheless do not display two-thirds of the information available—namely, the chemical shift anisotropies. In this section we present experimental results which illustrate the manner in which chemical shift scaling can be incorporated into a two-dimensional experiment to recover this information.

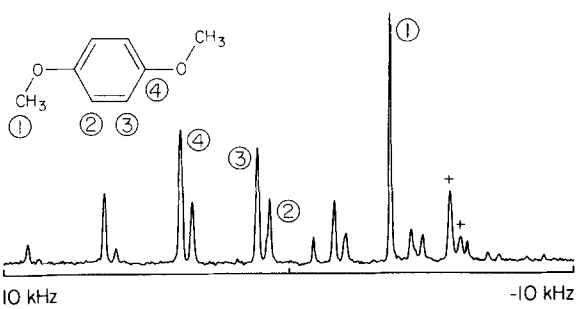

FIG. 6. MASS spectrum of ^{13}C natural abundance *para*-dimethoxybenzene. Cross polarization was used with a mixing time of 1 ms. The assignment of the centerbands is indicated according to Ref. 5. The spinner rate was adjusted to 2.70 kHz to get overlapping sideband patterns of the quaternary carbon and one of the aromatic nuclei. The two crosses mark lines due to a plastizer in the Kel-F from which the rotor was fabricated.

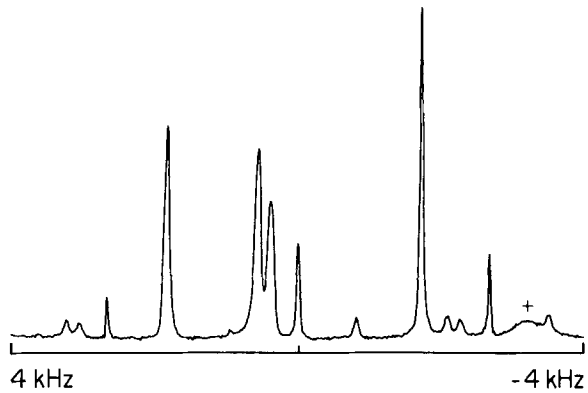

FIG. 7. Scaled MASS spectrum of *para*-dimethoxybenzene. The rf fields were 66 and 29 kHz for protons and ^{13}C. The scaling factor was $q = 0.50$, the cycle time 123.5 μs, and the spinner rate 2.70 kHz. The isotropic lines can be readily assigned. The downfield spinning sideband of the quaternary carbon is aliased. The impurity peaks have been broadened. ν_r artifacts show up clearly at 0 and $\pm \nu_r$.

The experimental situation which provides the rationale for this approach is illustrated in Figs. 6 and 7, which show ^{13}C spectra of *para*-dimethoxybenzene (PDMB). The normal MASS spectrum of this compound would exhibit four centerbands due to the methyl and three magnetically inequivalent aromatic carbons, together with their associated rotational sideband patterns. These are labeled 1–4 in Fig. 6. Moreover, at many spinning speeds these centerbands and sidebands would be resolved and both the isotropic and anisotropic shifts could be obtained. However, for the spectrum of Fig. 6 we have chosen ν_r equal to the separation of the centerbands belonging to carbons 3 and 4. Thus, the first upper sideband of carbon 4 is degenerate with the centerband from carbon 3, etc. Any attempt to evaluate the shift anisotropies from the sideband intensities in this case would obviously lead to erroneous results, because of this overlap. Furthermore, the simple 2*D* resolved experiment described previously[8] will not separate these centerbands and sidebands since $n\nu_r = \delta_i - \delta_j$ and the sideband patterns are intercalated.

Application of chemical shift scaling with $q = 0.5$ to the spectrum of Fig. 6 results in the spectrum shown in Fig. 7. Both the isotropic and anisotropic shifts have been reduced and the isotropic lines dominate the spectrum and are easily identified. There are resonances near both zero and $\pm \nu_r$ and thus, "ν_r artifacts" are clearly present. Pulse train imperfections also lead to a slight broadening of the lines apparent in the spectrum. The residual rotational sidebands in Fig. 7 are quite weak and it would clearly be difficult to obtain accurate information on the shift anisotropies. However, this information can be recovered with a 2*D* experiment.

In Fig. 8 we illustrate the pulse sequences required for this experiment. The preparation period consists of the customary Hartmann–Hahn cross polarization, and during the evolution period t_1, chemical shift scaling is employed to reduce the dispersion of the isotropic shifts. In addition, t_1 is incremented synchronously with the rotor, so that any residual sidebands are folded into the centerband. During t_2 we

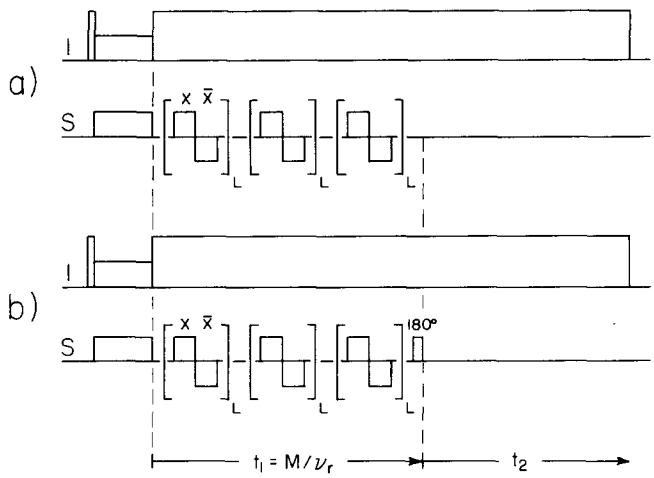

FIG. 8. Pulse sequences to generate the 2*D* resolved MASS spectrum shown in Fig. 9. Experiment (a) starts with Hartmann–Hahn cross polarization. During t_1, which is increased by $1/\nu_r$ in successive experiments, an integer number of pairs of joined pulses of opposite phase are applied to the *S* spins once every spinner revolution for uniform scaling of the chemical shifts. High power cw decoupling is applied to the abundant *I* spins. During t_2, which always begins at a rotational echo, samples are taken without restriction and under cw decoupling. Experiment (b) includes an additional 180° pulse at the end of t_1. Appropriate data processing of FIDS (a) and (b) allows one to obtain a 2*D* resolved MASS spectrum with pure absorption line shapes (see the text).

decouple and sample the magnetization in the customary fashion. In addition, as is shown in Fig. 8, we perform this experiment in a paired fashion in order to obtain pure absorption mode 2*D* spectra.[34] Specifically, a 180° pulse is added at the end of the evolution period in sequence (b). Subsequently we take the Fourier transforms of sum and difference of the FID's from (a) and (b), and add the real transform of the sum to the imaginary transform of the difference. This procedure has been discussed in detail elsewhere.[34]

A 2*D* resolved MASS ^{13}C spectrum of PDMB acquired using the pulse sequences of Fig. 8 is shown in Fig. 9, and the features in this spectrum are convincing. Specifically, the four sets of centerbands are clearly resolved and all of the fine structure in the MASS spectrum is preserved in the 2*D* spectrum. Note, for example, that the weak second sidebands of the methyl group are present and that the overlap in the centerband/sideband patterns in the ω_2 dimension from carbons 3 and 4 can be discerned. In the ω_1 dimension a scaling factor of 0.5 has been applied and therefore the lines of the methyl group and carbon 4 are aliased once. As mentioned previously this is not a problem since the isotropic shift is also present in ω_2 as redundant information. Thus, methyl and methylene lines will never be aliased into the aromatic/carbonyl region. In general we can allow for aliasing in ω_1 of those isotropic chemical shifts whose sideband patterns do not overlap in ω_2. Apart from a reduction in sensitivity, the loss of resolution in ω_1 introduced by the scaling process is of little consequence since in the 2*D* resolved spectrum the full resolution is present in ω_2. Therefore, even if scaled lines partially overlap in ω_1, they are separated in ω_2 with the normal MASS resolution.

V. CONCLUSIONS

To conclude, we have shown that the most efficient way to incorporate chemical shift scaling into 1*D* MASS experiments is to employ cw decoupling and scaling pulses which mismatch the Hartmann–Hahn condition. Furthermore, the uniformity of the experiment agrees remarkably with theoretical predictions, and therefore the experiment can in principle be used to regain the full signal intensity resident in the rotational sidebands without resorting to excessively high spinning speeds. This is an important feature of the experiment since it allows one to take advantage of the increased sensitivity available at high magnetic fields. The degree to which this statement is true will be determined by experimental variables like the fraction of signal that is lost by sampling between pulses, etc. In addition, we have also uncovered two interesting phenomena which we believe will be general features of multiple pulse/MASS experiments. First, when the multiple pulse cycle time is comparable to the reciprocal of the spinning rate, then combination sidebands and combination artifacts will appear in the spectra. The sidebands may prove useful for studying small shift tensors or other interactions which are attenuated by the spinning. Clearly their number and intensity will depend on the details of the particular experiment. Secondly, when NMR lines occur adjacent to the carrier or at multiples of the spinning frequency, then the zero and ν_r artifacts appear in the

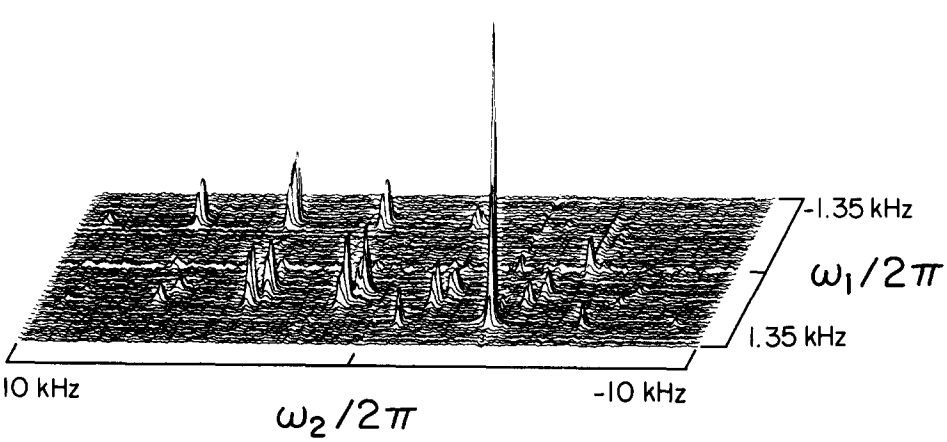

FIG. 9. 2*D* resolved MASS ^{13}C spectrum of *para*-dimethoxybenzene, obtained with the pulse scheme given in Fig. 8. The ω_1 domain contains the isotropic chemical shifts. The isotropic resonances of the methyl group and the quaternary carbon are aliased once, since the scaling factor of 0.50 could not fit them into the spectral width of the spinner rate (2.70 kHz). ν_r artifacts show up at $\omega_1 = 0$. In ω_2 direction, the normal MASS patterns are displayed the same way as in Fig. 5. The patterns of the quaternary carbon and the aromatic carbons are well separated and can be used to extract the chemical shift tensor elements. The experimental parameters are the same as in Fig. 6. Total acquisition time was 18 h and a 20 Hz Lorentzian line broadening has been applied to enhance sensitivity.

spectra. We have studied these in some detail here, and they have also been observed in ^{1}H multiple pulse MASS experiments. Thus, we believe they will be general features of these spectra. Finally, we have shown that scaling can be easily incorporated into a two-dimensional experiment which permits one to separate isotropic and anisotropic chemical shifts. The experiments utilize chemical shift scaling and synchronous sampling in t_1, and therefore there is considerable aliasing in this dimension of the $2D$ spectrum. Nevertheless, because of the redundant information present in the ω_2 dimension, a complete separation of the two interactions is possible. Experiments such as those described here as well as future developments in this field should pave the way for the routine use of MASS in solid state spectroscopy at high fields.

VI. ACKNOWLEDGMENTS

Thanks are accorded to M. Munowitz, S. Vega, E. Olejniczak, and J. Roberts for their stimulating conversations and assistance with various parts of this work. This research was supported by the National Institutes of Health (GM-23289, GM-23403, and RR-00995) and by the National Science Foundation (PCM-7901181 and DMR-8211416).

VII. APPENDIX

We include here a detailed procedure for implementing chemical shift scaling experiments. It is intended for the reader unfamiliar with solid state NMR. Our experience indicates that scaling can be set up in about half an hour if these instructions are followed closely. Typically we use a sample of ^{13}C enriched ethylene glycol and Na propionate for these adjustments.

With a liquid sample:

(1) Measure the width of the 90° pulses for the x and $\bar{x}$ channels with a $(90_x\tau\ 90_x\tau)_n$ sequence. The power level should be adjusted to mismatch the Hartmann–Hahn condition by a factor of at least 2.

(2) Adjust the phase difference between x and $\bar{x}$ to be 180° with a $(90_x\tau\ 90_{\bar{x}}\tau)_n$ sequence.

(3) Determine the proper timing for the scaling sequence from the tables in Ref. 14 and the measured 90° pulse widths.

(4) Fine adjust the pulse widths of the x and $\bar{x}$ channels to the proper scaling factor and minimum linewidth at an offset of about $\nu_{sc}/6$.

(5) Move to exact resonance and adjust the phases, pulse widths, and probe and power amplifier tuning (unless it is broad banded) until a zero frequency FID is observed. Satisfying this criterion insures that the scaling sequence is balanced with respect to the effective flip angles and phase transients in the amplifier/probe circuitry.

(6) Iterate (4) and (5) until the scaling factor is offset independent.

Then, with a spinning solid sample:

(7) Tune the probe to the frequency obtained in (5).

(8) Optimize the cross polarization MASS experiment and adjust ν_{sc} to be an integral multiple of ν_r if necessary.

(9) Begin scaling on the solid sample. The lines in a MASS spectrum are usually not narrow enough to optimize the sequence on resonance for zero frequency and therefore experiments at offset of $\pm\nu_{sc}/6$ should be performed. The rf on both channels should be adjusted to obtain the proper scaling factors and minimum linewidths.

(10) If the line positions in the scaled spectra are asymmetric with respect to positive and negative offsets then they should be symmetrized by means given in (5). A slight asymmetry does not influence the performance of the scaling sequences.

(11) Iterate (9) and (10).

[1] I. J. Lowe, Phys. Rev. Lett. **2**, 285 (1959).
[2] E. R. Andrew, Prog. Nucl. Magn. Reson. Spectrosc. **8**, 1 (1971).
[3] J. Schaefer and E. O. Stejskal, J. Am. Chem. Soc. **98**, 1031 (1976).
[4] E. Lippmaa, M. Alla and T. Tuherm, Proceedings of the XIXth Ampere Congress, Heidelberg, West Germany, 1976, p. 113.
[5] M. Maricq and J. S. Waugh, J. Chem. Phys. **70**, 3300 (1979).
[6] R. A. Haberkorn, J. Herzfeld, and R. G. Griffin, J. Am. Chem. Soc. **100**, 1296 (1978).
[7] J. Herzfeld and A. E. Berger, J. Chem. Phys. **73**, 6021 (1980).
[8] W. P. Aue, D. J. Ruben, and R. G. Griffin, J. Magn. Reson. **43**, 472 (1981).
[9] W. P. Aue, E. Bartholdi, and R. R. Ernst, J. Chem. Phys. **64**, 2229 (1976).
[10] W. T. Dixon, J. Magn. Reson. **44**, 220 (1981); J. Chem. Phys. **77**, 1800 (1982).
[11] J. D. Ellett, Jr. and J. S. Waugh, J. Chem. Phys. **51**, 2851 (1969).
[12] W. P. Aue, D. J. Ruben, and R. G. Griffin, J. Magn. Reson. **46**, 354 (1982).
[13] W. P. Aue and R. R. Ernst, J. Magn. Reson. **31**, 533 (1978).
[14] W. P. Aue, D. P. Burum, and R. R. Ernst, J. Magn. Reson. **38**, 375 (1980).
[15] W. P. Aue, Ph.D. thesis, Swiss Federal Institute of Technology, CH-8092, Zurich, Switzerland, 1979.
[16] A. J. Vega, A. D. English, and W. Mahler, J. Magn. Reson. **37**, 107 (1980).
[17] J. S. Waugh, L. M. Huber, and U. Haeberlen, Phys. Rev. Lett. **20**, 180 (1968).
[18] M. Mehring, *NMR Basic Principles and Progress* (Springer, New York, 1976).
[19] U. Haeberlen, *High Resolution NMR in Solids, Selective Averaging* (Academic, New York, 1976).
[20] M. Mehring, A. Pines, W. K. Rhim, and J. S. Waugh, J. Chem. Phys. **54**, 3239 (1971).
[21] H. Raber and M. Mehring, Chem. Phys. **26**, 123 (1977).
[22] P. van Hecke, H. W. Spiess, and U. Haeberlen, J. Magn. Reson. **22**, 103 (1976).
[23] J. A. Reimer and R. W. Vaughan, Chem. Phys. Lett. **63**, 163 (1979).
[24] J. A. Reimer and R. W. Vaughan, J. Magn. Reson. **41**, 483 (1980).
[25] A. Pines, M. G. Gibby, and J. S. Waugh, J. Chem. Phys. **59**, 569 (1973).
[26] S. R. Hartmann and E. L. Hahn, Phys. Rev. **128**, 2042 (1962).
[27] J. Herzfeld, R. G. Griffin, and R. A. Haberkorn, Biochemistry **17**, 2711 (1978).
[28] U. Haeberlen and J. S. Waugh, Phys. Rev. **175**, 453 (1968).
[29] E. T. Olejniczak, J. Roberts, S. Vega, and R. G. Griffin, J. Magn. Reson. (in press).
[30] Y. Yarim-Agaev, P. N. Tutunjian, and J. S. Waugh, J. Magn. Reson. **47**, 51 (1982).
[31] A. Bax, N. M. Szeverenyi, and G. E. Maciel, J. Magn. Reson. **51**, 400 (1983).
[32] J. A. Di Verdi and S. J. Opella, J. Chem. Phys. **75**, 5594 (1981).
[33] M. Munowitz, W. P. Aue, and R. G. Griffin, J. Chem. Phys. **77**, 1686 (1982).
[34] P. Bachmann, W. P. Aue, L. Müller, and R. R. Ernst, J. Magn. Reson. **28**, 29 (1977).